

Broadband Shock Associated Noise from Supersonic Jets Measured by a Ground Observer

Christopher K. W. Tam*

Florida State University, Tallahassee, Florida 32306

The theory of broadband shock associated noise from supersonic jets in flight previously developed in the nozzle-fixed coordinates is extended to the coordinate system of a stationary ground observer. The extended theory is relevant to community noise and aircraft certification noise prediction. Since the noise source is unaffected by which coordinate system of reference the radiated noise is measured, the same noise source model is retained in the present formulation. Only kinematic arguments are needed in the analysis. A formula for the noise power spectrum as measured by a ground observer is derived. The formula is applicable to hot as well as cold jets. This formula exhibits a form of Doppler shift in the noise spectrum. However, there is no high power convective amplification factor, as some other investigators have proposed.

I. Introduction

BROADBAND shock associated noise is an important component of supersonic jet noise. During the last several years a theory of this noise component has been developed by the present author.^{1,2} In these works the jets were assumed to be issued into a static environment. The theory is based on the large turbulence structures/instability waves shock cell interaction noise generation mechanism. The mean flow of a jet is highly unstable. It sustains downstream propagation large turbulence structures/instability waves. As these large turbulence structures/instability waves propagate through the quasiperiodic shock cell structure of an imperfectly expanded jet, coherent interactions take place. These interactions create unsteady disturbances. A part of these disturbances has supersonic phase velocity relative to the ambient speed of sound. This part is the source of broadband shock associated noise. Extensive comparisons between the calculated noise spectra, directivities, and near-field sound pressure level contours and the measurements of Norum and Seiner³ and Yu⁴ were carried out. Favorable overall agreements were found.

In a more recent paper the broadband shock associated noise theory was extended to include the effect of forward flight.⁵ The extended theory was developed in the nozzle-fixed reference frame. Changes in the noise sources due to the external flow as well as the convection effect of the external flow on the propagation of the radiated noise are accounted for in the theory. In the presence of a uniform mean flow outside the jet, the spacing of the shock cells is lengthened. The speed of propagation of the instability waves is increased, whereas the spatial growth and decay rates of the instability waves are reduced. These changes were incorporated into the extended theory. Since flight data were not available, the open wind-tunnel simulation noise measurements of Norum and Shearin^{6,7} were used for comparison and validation. In the simulation experiments the radiated sound has to traverse through the outer shear layer of the open wind tunnel before reaching the measurement microphones. In transmitting through the shear layer the noise spectrum and directivity are inevitably modified. In Ref. 5 the effects of the outer shear layers were approximated by those of a vortex sheet model. In this way the theory is self-contained without the necessity of applying shear layer corrections developed by various investi-

gators in the past using very localized source models. In the Norum and Shearin experiment, the wind tunnel was operated to a maximum simulated flight Mach number of 0.4. Numerical results indicated that the predicted noise levels, spectra, and directivities were in good agreement with the measured data over the entire range of simulated flight Mach numbers.

The extended theory⁵ was developed in the nozzle fixed coordinates. It is therefore convenient for comparisons with open-wind-tunnel noise measurements. However, for other applications, especially for the purposes of community noise analysis and aircraft noise certification, the nozzle-fixed coordinate system is not so relevant. A more important frame of reference is that of a ground-based observer. In the past a number of investigators^{8,9} developed formulas aimed at transforming the noise intensity and directivity of aircraft noise from a nozzle-fixed coordinate system to that of a ground observer in an overflight situation. Unfortunately, these formulas were based on highly localized compact noise source models or high-frequency approximations. The sources of broadband shock associated noise are noncompact and statistically random in nature. Because of these major differences, a straightforward application of these transformation formulas could lead to erroneous results. When a noise source of fixed frequency moves relative to a stationary observer, it is well known that the observed frequency undergoes a Doppler shift. If, however, the noise source is random, such as in the case of broadband shock associated noise, it is not clear that a simple Doppler shift correction to the noise spectrum calculated in the coordinate system moving with the source is all that is required. A detailed analysis of this question is advisable.

The objectives of this paper are twofold: 1) to develop a self-consistent broadband shock associated noise prediction formula as measured by a ground observer for supersonic jets in flight and 2) to extend the theory to high temperature jets.

The theory of Ref. 5 and the measurements of Refs. 6 and 8 were confined primarily to cold supersonic jets. To make the theory useful to aircraft noise prediction, it is important that the theory be extended to high temperature jets. In Ref. 2 a procedure by which the broadband shock associated noise theory developed originally for cold supersonic jets in a static environment may be modified for application to hot jets is provided. Here this procedure is used as the basis for extending the theory of Ref. 5 to high temperature jets.

In this work the sources of broadband shock associated noise are assumed to be the same as those in Ref. 5. Only kinematic arguments are used to determine the noise spectrum measured by a ground observer. Numerical results (see Sec. IV) indicate that a simple Doppler shift in frequency is not adequate to transform the noise spectrum from the nozzle-

Received Sept. 3, 1991; presented as Paper 92-0502 at the AIAA 30th Aerospace Sciences Meeting, Reno, NV, Jan. 6-9, 1992; revision received March 13, 1992; accepted for publication March 16, 1992. Copyright © 1992 by C. K. W. Tam. Published by the American Institute of Aeronautics and Astronautics, Inc., with permission.

*Professor, Department of Mathematics. Associate Fellow AIAA.

fixed coordinate system to the ground-based coordinate system. Further, according to the present prediction formula, there is no large convective amplification, as some previous point source model theories have suggested. These issues will be examined in depth in the concluding section of this paper.

II. Extension to Hot Jets

Consider a supersonic jet in flight. Let the fully expanded jet Mach number be M_j and the design Mach number of the convergent-divergent nozzle be M_d . The forward flight Mach number is M_f . The flow configuration in the nozzle fixed coordinate system is shown in Fig. 1. Let R be the radial distance from the center of the nozzle exit, ψ the inlet angle, and D the nozzle exit diameter. In Ref. 5 a formula [Eq. (3.7)] by which the broadband shock associated noise radiated in the direction of ψ can be calculated is provided. However, this formula is intended to be applicable to cold jets only. On following the procedure given in Ref. 2, this cold jet broadband shock associated noise formula may be modified for application to hot jets. Two types of corrections are required. The first type is the jet density correction. This can be accomplished by multiplying the original equation by the factor

$$(\rho_j/\rho_\infty) \left(1 + \frac{\gamma-1}{2} M_f^2\right)^{-1}$$

where ρ_j and ρ_∞ are the jet and ambient gas density, respectively, and γ is the ratio of specific heats. This factor is equal to unity for cold jets. For hot jets this factor reduces the noise intensity because of the lower jet density. The second type of corrections involve modifying the jet flow and instability wave parameters due to high jet temperature. The following temperature adjustments are recommended (for a flight Mach number < 0.5).

A. Convection Velocity of Large Turbulence Structures/Instability Waves

Let u_c , u_j , and u_f be the convection velocity of the instability waves, the jet velocity, and the flight velocity, respec-

$$f_m = \frac{u_c k_m / (2\pi)}{1 + M_c \{ [M_f(1 - M_f^2 \sin^2 \psi)^{1/2} + \cos \psi] / [(1 - M_f^2)(1 - M_f^2 \sin^2 \psi)^{1/2}] \}} \quad (7)$$

tively. If T_r is the total temperature of the jet and T_∞ is the ambient temperature, then u_c may be estimated by the following formula:

$$\frac{u_c}{u_j} = \begin{cases} [0.7 - 0.06(T_r/T_\infty - 1.0)](1 - u_f/u_j) + u_f/u_j & T_r/T_\infty > 1 \\ 0.7 + 0.3u_f/u_j & T_r/T_\infty < 1 \end{cases} \quad (1)$$

In Eq. (1) the coefficient 0.06 has been found empirically to give better results than the coefficient of Ref. 2 (0.025).

B. Half-Width of Similarity Noise Source

The half-width L is reduced by jet temperature. An extension of the formula of Ref. 5 is

$$L = 3.3 \left(\frac{x_c}{8.0}\right) \left[1.0 + \left(1.114 - 0.36 \frac{T_j}{T_\infty}\right) M_f\right] / D_j \quad (2)$$

where x_c , the core length of the jet, can be calculated by

$$\frac{x_c}{D_j} = \begin{cases} 4.3 + 1.2M_f^2, & T_j > T_\infty \\ 4.3 + 1.2 \left[M_f^2 + \left(1 - \frac{T_j}{T_\infty}\right) \right], & T_j < T_\infty \end{cases} \quad (3)$$

where T_j is the temperature of the jet, and D_j is the fully expanded jet diameter related to the nozzle exit diameter D by

$$\frac{D_j}{D} = \left\{ \frac{1 + [(\gamma-1)/2]M_d^2}{1 + [(\gamma-1)/2]M_f^2} \right\}^{(\gamma+1)/[4(\gamma-1)]} \left(\frac{M_d}{M_f}\right)^{1/2} \quad (4)$$

where M_d is the nozzle design Mach number.

C. Shock Cell Wave Numbers

The shock cell spacing of hot jets is reduced by forward flight. The wave number of the m th shock cell waveguide mode k_m may be calculated by

$$k_m(\text{hot jet at } M_f) = \frac{k_m(\text{cold jet at } M_f = 0)}{1.0 + (0.812 - 0.254T_j/T_\infty)M_f} \quad (5)$$

After the temperature modifications in Eq. (5) have been incorporated into Eq. (3.7) of Ref. 5, the following broadband shock associated noise power spectrum formula for hot supersonic jets in flight in the nozzle fixed coordinates is obtained:

$$S_{R-\infty}(R, \psi, f) = \frac{\bar{c} L^2 \bar{A}^2 A_j \rho_\infty^2 a_\infty^4 M_f^2}{R^2 (1 - M_f^2 \sin^2 \psi) f (f D_j / u_j) \{1 + [(\gamma-1)/2] M_f^2\}} \times \left\{ \sum_{m=1}^N \frac{1}{\sigma_m^2 J_1^2(\sigma_m)} \cdot \exp \left[- \left(\frac{f_m}{f} - 1 \right)^2 \right] \times \left(1 + M_c \frac{M_f (1 - M_f^2 \sin^2 \psi)^{1/2} + \cos \psi}{(1 - M_f^2)(1 - M_f^2 \sin^2 \psi)^{1/2}} \right)^2 \left(\frac{u_j}{u_c} \right)^2 \frac{L^2}{2 \ln 2} \right\} \quad (6)$$

where $\bar{c} = 2.65 \times 10^{-4} S_0 (S_0 = 0.35)$, $A_j = \pi D_j^2 / 4$, and a_∞ is the ambient speed of sound. J_1 is the Bessel function of order one, and σ_m is the m th zero of the Bessel function of order zero. In Eq. (6) the factor $f D_j / u_j$ in the denominator is to be replaced by S_0 whenever it is less than S_0 and

In formulating the broadband shock associated noise theory it has always been assumed that the convergent-divergent nozzle of M_d is perfectly manufactured. That is, when operating at a fully expanded Mach number $M_j = M_d$, there is no shock cell structure in the jet plume. In practice this is not always true, especially for hot jets. Because of various nozzle imperfections, a residual shock cell structure invariably exists so that even when the jet is operating nominally at the design Mach number there is still broadband shock associated noise. To account for this deviation from an ideal condition, one

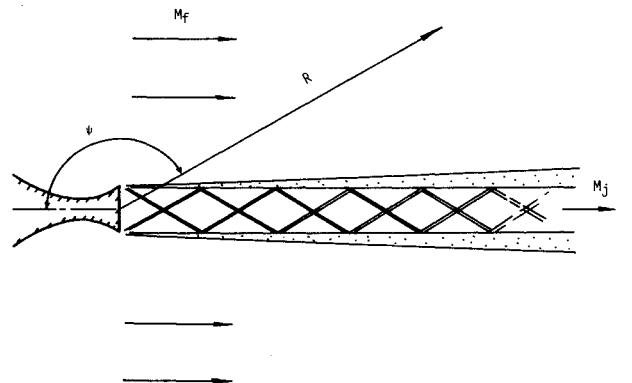


Fig. 1 Schematic diagram of the flow around a supersonic jet in flight in the nozzle-fixed coordinate system.

may incorporate empirically a residue shock cell strength ϵ in the parameter \bar{A}^2 of Eq. (6) as follows:

$$\bar{A}^2 = \begin{cases} \frac{[(M_j^2 - M_d^2)^2 + \epsilon] \left(\frac{D}{D_j}\right)^2 \left[1 + \frac{\gamma-1}{2} M_d^2\right]^2}{1 + 3 \left[(M_j^2 - M_d^2) \left(1 + \frac{\gamma-1}{2} M_d^2\right)\right]^3} & \text{(underexpanded jets)} \\ \frac{[(M_j^2 - M_d^2)^2 + \epsilon] \left[1 + \frac{\gamma-1}{2} M_d^2\right]^2}{1 + 6 \left[(M_d^2 - M_j^2) \left(1 + \frac{\gamma-1}{2} M_d^2\right)\right]^5} & \text{(overexpanded jets)} \end{cases} \quad (8)$$

where $\epsilon = 0$ corresponds to a $C - D$ nozzle without imperfections. Based on a number of numerical test cases, it is found that a value of $\epsilon = 0.03$ gives generally satisfactory results compared with experimental measurements. It should be noted that the residual shock cell strength is important only when the jet is operating closed to its nominal design condition.

Experimental data of broadband shock associated noise from hot supersonic jets are not readily available in the literature. After a fairly thorough search, only two sets of measurements^{10,11} were found. In the work of Tanna et al.¹⁰ the jets were discharged into a static environment. No forward flight effects were investigated. A 2-in. convergent nozzle was used in the experiments. To suppress the screech tones, metal taps were inserted around the nozzle lip. From the measurements of Norum and Seiner³ it is known that such taps have the unintended side effects of also reducing the peak level of broad-

band shock associated noise. This point must be borne in mind when comparing calculated results with measurements. Tanna et al.¹⁰ presented their data as 200-Hz band sound pressure level spectra. Figures 2a-2d show typical comparisons between calculated noise spectra of Eq. (6) and experimental measurements in the forward arc. As can be seen the peak frequencies of broadband shock associated noise for this high-temperature jet (total temperature = 1307°R) are well predicted. A maximum of $N = 35$ modes are used in the calculations. The dips in the predicted spectra (e.g., ~ 7 kHz) in Fig. 2a have been noted and discussed in Ref. 1. The calculated peak noise levels are generally 3 dB higher than the measurements. The main part of this discrepancy is believed to be due to the effects of the taps used in the experiments. A quantitative estimate of this effect is desirable but is unavailable at the present time.

Another set of broadband shock noise data available for comparison was measured by Yamamoto et al.¹¹ In these more recent experiments the jets were operated at even higher total temperature. Both conical and convergent-divergent nozzles were used. In addition, open-wind-tunnel forward-flight simulation noise measurements were made. Figures 3a-3c show typical comparisons between calculated results and measurements. For this run the total temperature of the jet was 1718°R and a convergent nozzle of 5.094 in. in diameter was used. As is readily seen overall there is good agreement between predictions and measurements. This is true both in spectral distribution and in absolute level. To simulate the effect of forward flight, an open wind tunnel of 48-in. in diameter was used in the experiment of Yamamoto et al. In all of the flight simulation measurements the wind-tunnel speed was set at 400 ft/s. To be able to use these measurements to test the validity of the hot jet shock noise theory, a vortex sheet wind-tunnel model similar to that in Ref. 5 was adopted in the analysis. The extended theory allows a direct comparison between the calculated results and microphone measure-

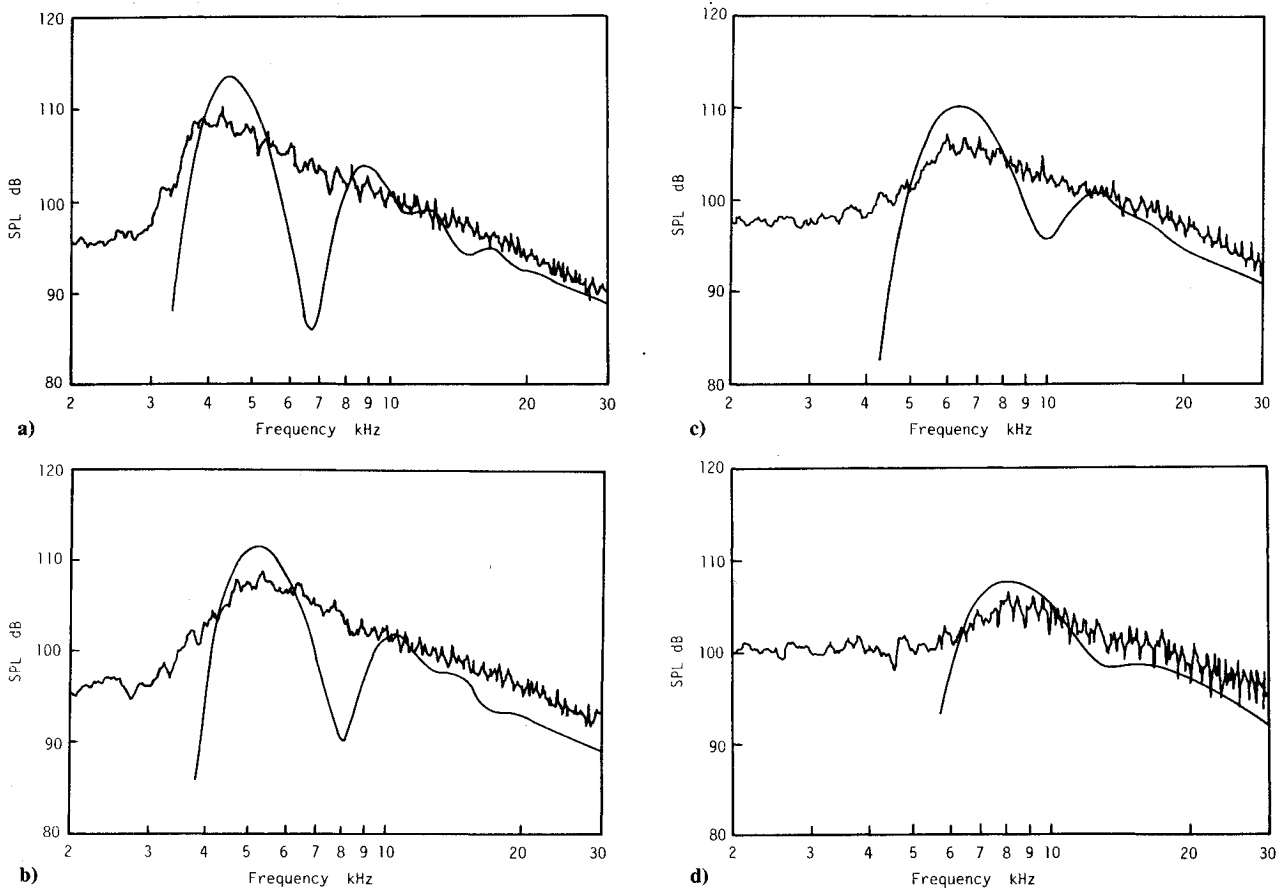


Fig. 2 Comparisons between calculated spectra and the experimental measurements of Ref. 10 ($M_j = 1.487$, $M_d = 1.0$, $T_r = 1307^\circ\text{R}$, $T_r/T_\infty = 2.524$, $\gamma = 1.35$): a) $\psi = 45$ deg; b) $\psi = 60$ deg; c) $\psi = 75$ deg; d) $\psi = 90$ deg.

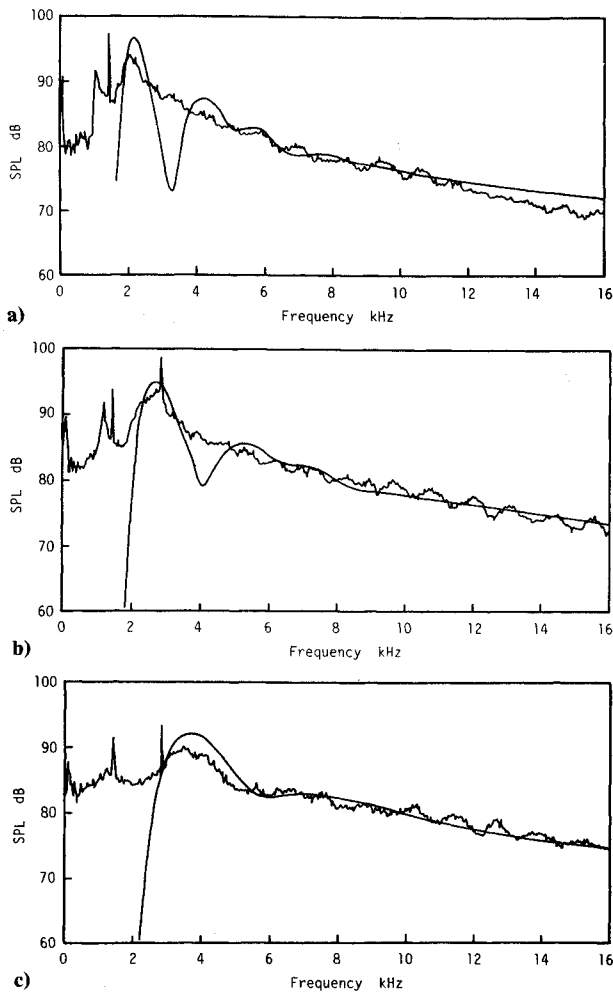


Fig. 3 Comparisons between calculated results and measurements of Ref. 11 ($M_j = 1.336$, $M_d = 1.0$, $T_r = 1718^\circ\text{R}$, $T_r/T_\infty = 3.31$, $\gamma = 1.36$): a) $\psi = 50$ deg; b) $\psi = 70$ deg; c) $\psi = 90$ deg.

ments. Figures 4a–4c show the calculated and measured shock noise spectra at $\psi = 50, 70$, and 90 deg for a Mach 1.439 jet at 1710°R total temperature. As has been discussed in Ref. 5 for cold jets, one effect of the simulated forward flight is the shifting of the spectral peak to a lower frequency. The calculated results appear to match this frequency shift well. In addition, the calculated peak levels and the spectral shapes are in good agreement with measurements. Although not reported here, comparisons between calculated results and all of the measured hot jet data of Ref. 11 with and without forward-flight simulation had been carried out. Overall, favorable agreements were found.

III. Shock Noise Measured by a Ground Observer

In Ref. 5 a broadband shock associated noise theory from supersonic jets in forward flight is developed. This theory is an extension of earlier works.^{1,2} In this theory the random acoustic noise field generated by the interaction of the large turbulence structures/instability waves and the shock cell structure of the jet flow is found in a nozzle-fixed coordinate system. In this section a formula for the power spectrum of this same noise field as measured by a ground observer is derived. Since the noise field is unchanged regardless of whether it is measured in the nozzle-fixed or the ground-fixed coordinates, only a kinematic analysis is needed for this purpose.

Let (r, ϕ, x) be the coordinates of a nozzle-fixed cylindrical coordinate system centered at the nozzle exit with the x axis pointing in the direction of the jet flow as shown in Fig. 5. For reference purpose let (R, θ, ϕ) be the corresponding spherical

coordinates, where θ is the polar angle measured from the x axis, and θ is the supplement of the inlet angle ψ . The relationships between the two coordinate systems are

$$r = R \sin \theta, \quad x = R \cos \theta, \quad \phi = \phi \quad (9)$$

Relative to this frame of reference, a ground observer moves with constant velocity u_f in the x direction, where u_f is the flight velocity. Consider a ground observer located at (r, ϕ, x) at time t . The observer measures the pressure fluctuations associated with the random noise field generated by the jet. Let τ_{eff} be the effective correlation time of the random acoustic wave field measured by the ground observer. In the time interval τ_{eff} the observer moves a distance $\tau_{\text{eff}}u_f$ in the x direction. It will be assumed that the observer is in the far field, so that $\tau_{\text{eff}}u_f/R \ll 1$. This implies that $\delta\theta = u_f\tau_{\text{eff}} \sin \theta/R$ and $\delta R/R = u_f\tau_{\text{eff}} \cos \theta/R$ ($\delta\theta$ and δR are the change in the ground observer's coordinates in the time interval τ_{eff}) are very small. In other words, the change in θ and R over the time interval τ_{eff} is negligible.

With respect to the nozzle-fixed coordinate system, a formula for the pressure of the random broadband shock associated noise field is provided in Ref. 5. In this paper the same notation as that in Ref. 5 will be used. The present effort is, first, to calculate the autocorrelation function as the ground observer would have measured it. Then the noise power spectrum is obtained by taking its Fourier transform. According to Ref. 5, the pressure of the noise field at the location of the

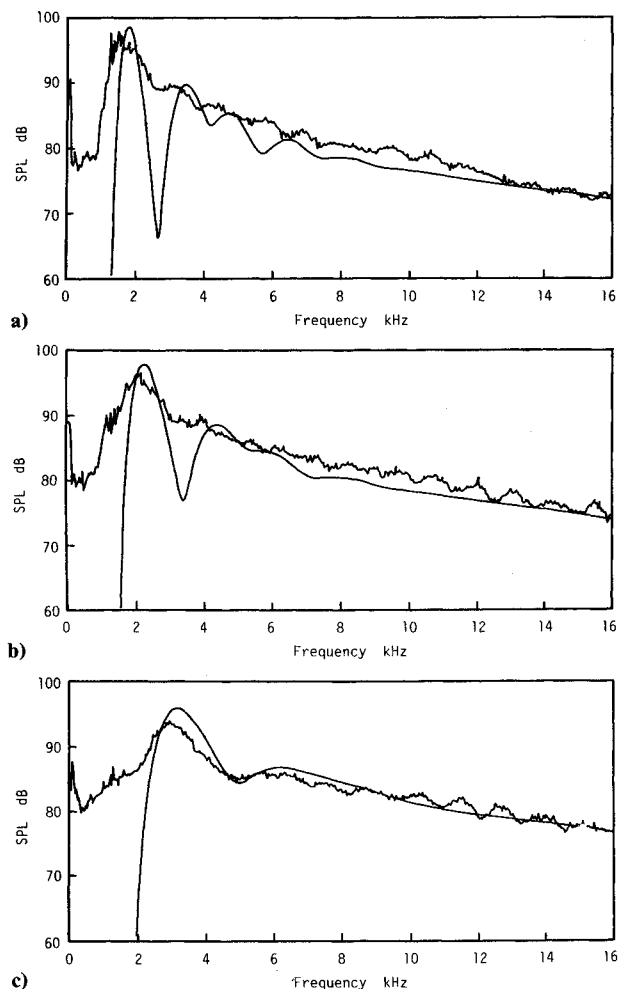


Fig. 4 Comparisons between calculated results and measurements of Ref. 11 ($M_j = 1.439$, $M_d = 1.0$, $M_f = 0.358$, $T_r = 1710^\circ\text{R}$, $T_r/T_\infty = 3.295$, $\gamma = 1.366$): a) $\psi = 50$ deg; b) $\psi = 70$ deg; c) $\psi = 90$ deg.

ground observer at time t associated with the m th shock cell waveguide mode is given by

$$p_m(r, \phi, x, t) = \sum_{n=-\infty}^{\infty} \int_{-\infty}^{\infty} a_n(\omega) g_{nm}(\eta, \omega) H_n^{(1)}[i\nu(\eta, \omega)r] \exp[i(\eta x + n\phi - \omega t) + i(n+1)\pi/2] d\eta d\omega \quad (10)$$

where

$$g_{nm}(\eta, \omega) = \frac{1}{2\pi} \int_{-\infty}^{\infty} A_{nm}(x, \omega) \exp[i(\Theta_n - \Psi_m)/\epsilon - i\eta x] dx \quad (11)$$

$$g_{nm}(-\eta, -\omega) = g_{nm}^*(\eta, \omega)$$

$$\nu(\eta, \omega) = [\eta^2 - (\omega - u_f \eta)^2/a_\infty^2]^{1/2}$$

$$-\pi/2 \leq \arg \nu \leq \pi/2 \quad (12)$$

$$\langle a_n(\omega) a_{n'}(\omega') \rangle = \frac{1}{2} \bar{D} \left(\frac{R_j}{u_j} \right) \delta(\omega + \omega') \delta_{n, -n'} \quad (13)$$

where the asterisk denotes a complex conjugate. In Eq. (12) the equality sign on the right (left) is to be deleted if $\omega > 0$ ($\omega < 0$). $H_n^{(1)}(\cdot)$ is the n th-order Hankel function of the first kind, $\langle \rangle$ denotes the ensemble average, and $\delta(\omega + \omega')$ and $\delta_{n, -n'}$ are the delta function and Kronecker delta, respectively. At a later time $t + \tau$ the ground observer would have moved to the point $(r, \phi, x + u_f \tau)$. The pressure of the random acoustic field at this point and time is

$$p_m(r, \phi, x + u_f \tau, t + \tau) = \sum_{n'=-\infty}^{\infty} \int_{-\infty}^{\infty} a_{n'}(\omega') g_{n'm}(\eta', \omega') H_{n'}^{(1)}[i\nu(\eta', \omega')r] \exp[i(\eta' x + n' \phi - \omega' t) + i(\eta' u_f - \omega') \tau] \exp[i(n' + 1)\pi/2] d\eta' d\omega' \quad (14)$$

By means of Eqs. (9) and (14) the autocorrelation function of the acoustic field as measured by the ground observer can be calculated:

$$\langle p_m(r, \phi, x, t) p_m(r, \phi, x + u_f \tau, t + \tau) \rangle = \sum_{n=-\infty}^{\infty} \sum_{n'=-\infty}^{\infty} \int_{-\infty}^{\infty} \int_{-\infty}^{\infty} \langle a_n(\omega) a_{n'}(\omega') \rangle \cdot g_{nm}(\eta, \omega) g_{n'm}(\eta', \omega') H_n^{(1)}[i\nu(\eta, \omega)r] H_{n'}^{(1)}[i\nu(\eta', \omega')r] \cdot \exp\{i[(\eta + \eta')x + (n + n')\phi - (\omega + \omega')t + (\eta' u_f - \omega')\tau + (n + n')\pi + \pi]\} d\eta d\eta' d\omega d\omega' \quad (15)$$

Upon substituting the ensemble average property of the stochastic amplitude function a_n [Eq. (13)] into Eq. (15) and summing over the Kronecker delta $\delta_{n, -n'}$ and integrating over the delta function $\delta(\omega + \omega')$, it is straightforward to find

$$\langle p_m(r, \phi, x, t) p_m(r, \phi, x + u_f \tau, t + \tau) \rangle = \frac{1}{2} \bar{D} \left(\frac{R_j}{u_j} \right) \sum_{n=-\infty}^{\infty} \int_{-\infty}^{\infty} \int_{-\infty}^{\infty} g_{nm}(\eta', \omega') \cdot g_{nm}^*(\eta, \omega') H_n^{(1)}[i\nu(\eta', \omega')r] H_n^{(1)*}[i\nu(\eta, \omega')r] \cdot \exp\{i[(\eta' - \eta)x + (\eta' u_f - \omega')\tau]\} d\eta d\eta' d\omega' \quad (16)$$

For a ground observer in the far field the η and η' integrals of Eq. (16) may be evaluated asymptotically. On replacing the Hankel function by its asymptotic form and then switching to

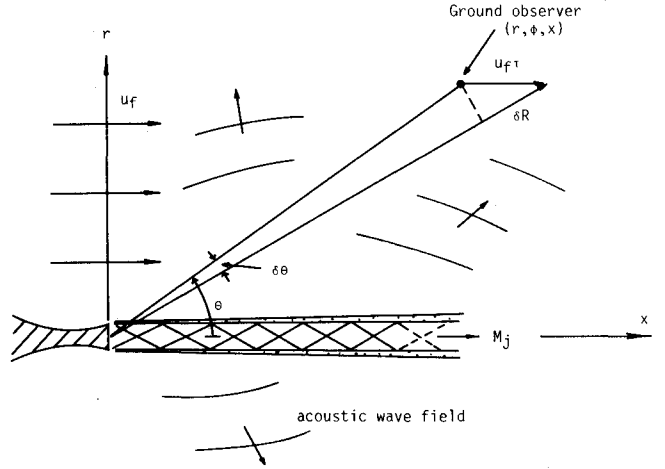


Fig. 5 Coordinates of a ground observer relative to the supersonic jet in the nozzle fixed coordinate system.

spherical polar coordinates according to Eq. (8), the following is found:

$$\lim_{R \rightarrow \infty} \int_{-\infty}^{\infty} g_{nm}(\eta', \omega') H_n^{(1)}[i\nu(\eta', \omega')r] e^{i\eta'(x + u_f \tau)} d\eta' \sim \lim_{R \rightarrow \infty} \int_{-\infty}^{\infty} g_{nm}(\eta', \omega') \cdot \left(\frac{2}{i\pi R \sin \theta} \right)^{1/2} \cdot [(\exp\{[-\nu(\eta', \omega') \sin \theta + i\eta' \cos \theta]R\}) \cdot \exp\{i\eta' u_f \tau - i(n + 1/2)\pi/2\}] / [\nu(\eta', \omega')]^{1/2} d\eta' \quad (17)$$

The preceding integral may be evaluated by the method of steepest descents.¹² It is straightforward to find that the saddle point η'_s is given by

$$\eta'_s = \frac{\omega'}{a_\infty} \left[\frac{\cos \theta}{(1 - M_f^2 \sin^2 \theta)^{1/2}} - M_f \right] \frac{1}{1 - M_f^2} \quad (18)$$

where $M_f = u_f/a_\infty$ is the forward-flight Mach number. Upon applying the method of steepest descents to Eq. (17), the integral is evaluated:

$$\lim_{R \rightarrow \infty} \int_{-\infty}^{\infty} g_{nm}(\eta', \omega') H_n^{(1)}[i\nu(\eta', \omega')r] e^{i\eta'(x + u_f \tau)} d\eta' \sim g_{nm}(\eta'_s, \omega') \cdot \frac{2}{R(1 - M_f^2 \sin^2 \theta)^{1/2}} \exp\left\{i \left[\frac{\omega' R/a_\infty}{M_f \cos \theta - (1 - M_f^2 \sin^2 \theta)^{1/2}} + \eta'_s u_f \tau - (n + 1)\pi/2 \right]\right\} \quad (19)$$

A similar formula for the η integral can easily be derived. On substitution into Eq. (16) the autocorrelation function becomes

$$\langle p_m(r, \phi, x, t) p_m(r, \phi, x + u_f \tau, t + \tau) \rangle = \frac{1}{2} \bar{D} \left(\frac{R_j}{u_j} \right) \sum_{n=-\infty}^{\infty} \int_{-\infty}^{\infty} \frac{4 |g_{nm}(\eta'_s, \omega')|^2}{R^2 (1 - M_f^2 \sin^2 \theta)} \cdot e^{i(\eta'_s u_f - \omega')\tau} d\omega' \quad (20)$$

Now the power spectrum is the Fourier transform of the autocorrelation function. The power spectrum of broadband shock noise associated with the m th shock cell waveguide mode measured by the ground observer is therefore given by

$$S_m(\omega) = \frac{1}{2\pi} \int_{-\infty}^{\infty} \langle p_m(r, \phi, x, t) p_m(r, \phi, x + u_f \tau, t + \tau) \rangle e^{-i\omega \tau} d\tau \quad (21)$$

After substitution of Eq. (20) into Eq. (21) the integration over τ can be carried out independently of the function g_{nm} . The result is a delta function. Upon integrating ω' over the delta function, the expression for the broadband shock associated noise power spectrum generated by the m th shock cell waveguide mode is (assuming axisymmetric sources and sound field as in Ref. 5)

$$S_m(\omega) = 2 \bar{D} \left(\frac{R_j}{u_j} \right) \frac{M_f \cos \theta + (1 - M_f^2 \sin^2 \theta)^{1/2}}{R^2 (1 - M_f^2 \sin^2 \theta)^{1/2}} |g_m(\eta'_s, \omega')|^2 \quad (22)$$

where

$$\omega' = \omega [M_f \cos \theta + (1 - M_f^2 \sin^2 \theta)^{1/2}] (1 - M_f^2 \sin^2 \theta)^{1/2}$$

Following Refs. 2 and 5, we will adopt the similarity source model first introduced in Ref. 1. This provides the following explicit expression for g_m :

$$|g_m(\eta'_s, \omega')| = \frac{\bar{E}L}{2(\pi \ln 2)^{1/2}} \frac{\rho_\infty a_\infty \bar{A} R_j^{1/2} u_j^{3/2} (\pi S_0)^{1/2}}{\sigma_m J_1(\sigma_m) (\omega')^{1/2} (\omega' R_j / u_j)^{1/2}} \times \exp \left(- \left(\frac{\omega_m}{\omega'} - 1 \right)^2 \left\{ 1 + \frac{u_c}{a_\infty} \times \left[\frac{M_f (1 - M_f^2 \sin^2 \theta)^{1/2} - \cos \theta}{(1 - M_f^2)(1 - M_f^2 \sin^2 \theta)^{1/2}} \right]^2 \left(\frac{u_j L}{u_c} \right)^2 \frac{1}{4 \ln 2} \right\} \right) \quad (23)$$

where the factor $(\omega' R_j / u_j)^{1/2}$ is to be replaced by $(\pi S_0)^{1/2}$, $S_0 = 0.35$, whenever $\omega' R_j / u_j > \pi S_0$ and

$$\omega_m = (u_c k_m) \left(\left(1 + \frac{u_c}{a_\infty} \{ [M_f (1 - M_f^2 \sin^2 \theta)^{1/2} - \cos \theta] / [(1 - M_f^2)(1 - M_f^2 \sin^2 \theta)^{1/2}] \} \right) \right) \quad (24)$$

Finally, by summing up the contributions over all the shock cell waveguide modes (i.e., $S = \sum_m S_m$) and incorporating the temperature correction factor (see Sec. II), the spectrum of broadband shock associated noise measured by the ground observer is given by

$$S(R, \psi, f) = \frac{\bar{c} L^2 \bar{A}^2 A_j \rho_\infty^2 a_\infty^4 M_f^2}{R^2 (1 - M_f^2 \sin^2 \psi) f (f' D_j / u_j) \{ 1 + [(\gamma - 1)/2] M_f^2 \}} \times \left(\sum_{m=1}^N \frac{1}{\sigma_m^2 J_1^2(\sigma_m)} \cdot \exp \left\{ - \left(\frac{f_m}{f} - 1 \right)^2 \right\} \right) \times \left[1 + M_c \frac{M_f (1 - M_f^2 \sin^2 \psi)^{1/2} + \cos \psi}{(1 - M_f^2)(1 - M_f^2 \sin^2 \psi)^{1/2}} \right]^2 \left(\frac{u_j}{u_c} \right)^2 \frac{L^2}{2 \ln 2} \quad (25)$$

where $f' = f [(1 - M_f^2 \sin^2 \psi)^{1/2} - M_f \cos \psi] (1 - M_f^2 \sin^2 \psi)^{1/2}$. In Eq. (25) the factor $(f' D_j / u_j)$ is to be replaced by S_0 ($S_0 = 0.35$) whenever it is less than S_0 and

$$\hat{f}_m = [u_c k_m / (2\pi)] / [(z - M_f \cos \psi) z + M_c (M_f z + \cos \psi) (z + M_f \cos \psi)^{-1}] \quad (26)$$

$$z = (1 - M_f^2 \sin^2 \psi)^{1/2}$$

The parameters in Eqs. (25) and (26) are the same as those in Eq. (6).

Equation (25) is the principal result of this paper. This formula for a ground observer at (R, θ) is almost the same as that in Eq. (6) evaluated at the same point in space (but moving with the jet). The major difference is in the formula for \hat{f}_m [Eq. (26)] vs f_m [Eq. (7)]. The change from f_m to \hat{f}_m

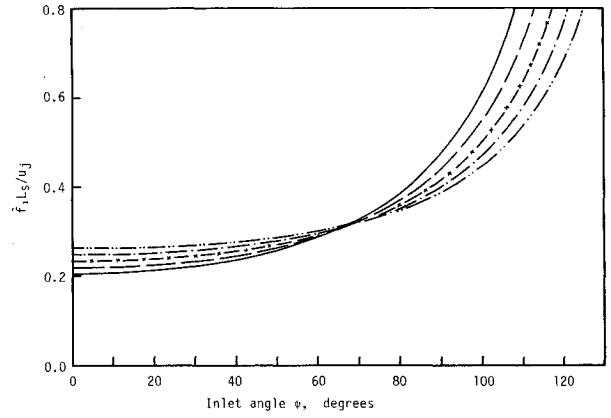


Fig. 6 Peak frequency of broadband shock associated noise measured by a ground observer ($M_j = 1.5$, $T_r = 2500^\circ \text{R}$, $T_\infty = 520^\circ \text{R}$). —, $M_f = 0.0$; - - -, $M_f = 0.1$; -x-x-, $M_f = 0.2$; ····, $M_f = 0.3$; - · - ·, $M_f = 0.4$.

amounts to a form of Doppler shift in the frequency of the spectrum. For a low flight Mach number (neglecting M_f^2 terms) they are related by

$$\hat{f}_m = f_m (1 + M_f \cos \psi) \quad (27)$$

Since the spectrum given by Eq. (6) peaks nearly at $f = f_m$ and the spectrum given by Eq. (26) peaks nearly at \hat{f}_m , Eq. (27) is simply a statement of the often-used Doppler shift formula. At a higher flight Mach number Eq. (27) is not adequate and Eq. (26) should be used.

Figure 6 shows an example of the variation of the peak frequency \hat{f}_1 ($m = 1$, the main peak of the spectrum) with flight Mach number for a hot jet at 2500°R total temperature and a jet Mach number 1.5. In this figure \hat{f}_1 is nondimensionalized with respect to the shock cell spacing L_s at static condition ($M_f = 0$) and u_j , the jet velocity. As forward flight speed increases, the peak frequency measured by a ground observer in the forward direction increases, whereas a ground observer in the rear arc would record a downward shift of the peak frequency. The trend is similar to that of Eq. (27). However, unlike the prediction of Eq. (27), the direction without any shift of the peak frequency is not at $\psi = 90$ deg but at ~ 65 deg. Also, the magnitude of the frequency shift is much larger in the rear arc than in the forward arc. The usefulness of Eq. (27) for broadband shock associated noise prediction is therefore very limited, and is primarily restricted to a very low flight Mach number.

Note: In Eq. (25) ψ and R are the angle and distance measured at reception time. If ψ_e and R_e are the emission angle and distance measured at emission time then they are related by

$$R = R_e (1 + M_f^2 - 2M_f \cos \psi_e)^{1/2}$$

$$\psi = \begin{cases} \sin^{-1} [\sin \psi_e / (R/R_e)], & \text{if } \cos \psi_e > M_f \\ \pi - \sin^{-1} [\sin \psi_e / (R/R_e)], & \text{otherwise} \end{cases}$$

IV. Discussion

It is worthwhile to point out that in Ref. 5 it was explicitly assumed that the exterior wall of the nozzle was covered by a boundary layer that was quite thick at the nozzle exit. The thick boundary-layer assumption is important because it allows one to use the same formula to estimate the shock cell strength in flight as in the static case. Equation (25) is based on the source model of Ref. 5. Thus, it should only be applied to supersonic jets with a thick external boundary layer at the nozzle exit.

Classical theory¹³ of a moving point source and more recent theory based on somewhat more realistic simple sources in

motion¹⁴ suggest that the noise radiated increases by a factor (usually referred to as convective amplification factor) of

$$(1 - M_f \cos \psi)^{-4} \quad (28)$$

due to forward flight. Others researchers,^{8,9} using localized noise source models and ray acoustics (high frequency approximation), derived similar noise amplification factor in more general situations. As a result, it has been interpreted by some investigators that such a convective amplification factor should also apply to broadband shock associated noise. When the flight Mach number is closed to unity, this factor is exceedingly large for directions in the forward arc. If it is used to transform the noise calculated or measured in the nozzle fixed coordinates to the ground observer's coordinates, the increase in noise level is enormous. However, Eq. (25), which gives the noise spectrum measured by a ground observer, does not contain such convective amplification factor. Thus, it would not predict a huge increase in broadband shock associated noise in the forward arc. Equation (25) was derived using the large turbulent structures/instability waves shock cell interaction noise source model. The noise source is noncompact and differs completely from sources used to derive the convective amplification factor of Eq. (28). Unfortunately, at the present time, no flight data of good quality are available to distinguish whether a large convective amplification exists as $M_f \rightarrow 1$. Therefore, it is hoped that such data will soon become available to settle this "convective amplification" puzzle once and for all.

Acknowledgment

This work was supported by NASA Langley Research Center Grant NAG1-421.

References

¹Tam, C. K. W., "Stochastic Model Theory of Broadband Shock-Associated Noise from Supersonic Jets," *Journal of Sound and Vi-*

bration, Vol. 116, No. 2, 1987, pp. 265-302.

²Tam, C. K. W., "Broadband Shock Associated Noise of Moderately Imperfectly Expanded Supersonic Jets," *Journal of Sound and Vibration*, Vol. 140, No. 1, 1990, pp. 55-71.

³Norum, T. D., and Seiner, J. M., "Measurements of Mean Static Pressure and Far Field Acoustics of Shock-containing Supersonic Jets," NASA TM 84521, Sept. 1983.

⁴Yu, J. C., "Investigation of the Noise Fields of Supersonic Axisymmetric Jet Flows," Ph.D. Dissertation, Department of Mechanical Engineering, Syracuse Univ., Syracuse, NY, April 1971.

⁵Tam, C. K. W., "Broadband Shock Associated Noise from Supersonic Jets in Flight," *Journal of Sound and Vibration*, Vol. 151, No. 1, 1991, pp. 131-147.

⁶Norum, T. D., and Shearin, J. G., "Shock Noise from Supersonic Jets in Simulated Flight to Mach 0.4," AIAA Paper 86-1845, July 1986.

⁷Norum, T. D., and Shearin, J. G., "Shock Structure and Noise of Supersonic Jets in Simulated Flight to Mach 0.4," NASA TP 3785, Feb. 1988.

⁸Larson, R. S., "Convective Amplification of Gas Turbine Engine Internal Noise Sources," *Journal of Sound and Vibration*, Vol. 74, No. 1, 1981, pp. 123-137.

⁹Amiet, R. K., "Correction of Fan Noise for Effects of Forward Flight," *Journal of Sound and Vibration*, Vol. 89, No. 2, 1983, pp. 243-259.

¹⁰Tanna, H. K., Dean, P. D., and Burrin, R. H., "The Generation and Radiation of Supersonic Jet Noise. Volume IV, Shock Associated Noise Data," Air Force Aero-Propulsion Lab., AFAPL-TR-76-65, Wright-Patterson AFB, OH, Sept. 1976.

¹¹Yamamoto, K., Brausch, J. F., Janardan, B. A., Hoerst, D. J., Price, A. O., and Knott, P. R., "Experiment Investigation of Shock-Cell Noise Reduction for Single-Stream Nozzles in Simulated Flight, Comprehensive Data Report, Volume 1," NASA CR-168234, May 1984.

¹²Wong, R., *Asymptotic Approximations of Integrals*, Academic, San Diego, CA, 1989, Chap. 2.

¹³Morse, P. M., and Ingard, K. U., *Theoretical Acoustics*, McGraw-Hill, New York, 1968, Chap. 1.

¹⁴Dowling, A., "Convective Amplification of Real Simple Sources," *Journal of Fluid Mechanics*, Vol. 74, Pt. 3, 1976, pp. 529-546.